

# Cracking in Quasi-Brittle Materials Using Isotropic Damage Mechanics

Tobias Gasch<sup>\*1</sup> and Anders Ansell<sup>1</sup>

<sup>1</sup>KTH Royal Institute of Technology, Department of Civil and Architectural Engineering

\*Corresponding author: Brinellvägen 23, SE-100 44 Stockholm, Sweden, tobias.gasch@byv.kth.se

**Abstract:** An extension of the Solid mechanics interface in Comsol Multiphysics is presented to analyse localized deformations of quasi-brittle materials, for example cracking in concrete. This is achieved by implementing an isotropic damage mechanics constitutive law, which is combined with both a local and a non-local regularization technique to ensure mesh objectivity. The implementation is made using equation based modelling and modification of built-in features. To facilitate easier use of the model, a custom user interface is constructed using the Physics Builder. Lastly, the implemented model is validated using examples of both plain and reinforced concrete, with two examples taken from the literature. Overall the simulation results are in good agreement with the experimental observations.

**Keywords:** Concrete, Cracking, Solid mechanics, Damage, Strain localization

## 1. Introduction

A common property of quasi-brittle materials such as concrete is that they exhibit a strain softening behaviour after their peak load is reached. This can be compared to the strain hardening behaviour of e.g. metals or perfectly brittle materials that lose their load carrying capacity instantly after the peak load is reached. This strain softening behaviour has proven to be a significant challenge to account for when using numerical analysis methods. It gives rise to a strong size effect [1] and consequently a dependency on the discretization as the strains localize and form cracks. Over the years several methods have been proposed in the literature to overcome this issue. One way to categorize them is to look at how the modelled cracks affect the displacement field [2]. Using this criterion, three categories can be distinguished, as seen in Fig. 1. Category 1 implies a jump in the displacement field, and consequently a singularity in the strain field suggesting that cracking is localized to element boundaries. Category 2 implies a discontinuity in the displacement field and hence a jump in the strain field. With such methods

cracking becomes localized in single rows of elements or rows of Gauss points. In the third category, both the displacement and the strain field remain continuous and cracking is typically distributed over several elements.

In this paper, an isotropic scalar damage constitutive law is implemented in Comsol Multiphysics and combined with the Solid mechanics interface. Firstly, by introducing the element size into the constitutive law, a model of category 2 from Fig. 1 is obtained. Secondly, it is shown how to obtain a model of category 3 by only making minor modifications to the former model, both in its mathematical structure and implementation in Comsol Multiphysics. Although applicable to any material exhibiting quasi-brittle fracture, the models are here exemplified using concrete using examples from the literature. The differences between the two versions of the constitutive law are shown for plain concrete whereas the first version is applied to reinforced concrete.

## 2. Isotropic Damage Mechanics

The model here implemented is an extension of the Solid mechanics interface in Comsol Multiphysics which is based on the standard momentum balance equation. For simplicity, inertial effects are here neglected and displacements and strains assumed to remain small. This leads to the following governing equations:

$$\nabla \cdot \boldsymbol{\sigma} + \mathbf{F}_V = 0 \quad (1)$$

$$\boldsymbol{\epsilon} = \frac{1}{2} (\nabla \mathbf{u} + \nabla \mathbf{u}^T) \quad (2)$$

In Eq. (1),  $\boldsymbol{\sigma}$  is the stress tensor and  $\mathbf{F}_V$  contains the body forces, while in Eq. (2),  $\boldsymbol{\epsilon}$  is the strain tensor and  $\mathbf{u}$  are the displacements. These two equations are then complemented by appropriate boundary conditions and a constitutive law relating stresses and strains to complete the problem definition.

In the analysis of localized deformations of strain softening materials such as cracking of concrete, a popular class of constitutive laws are

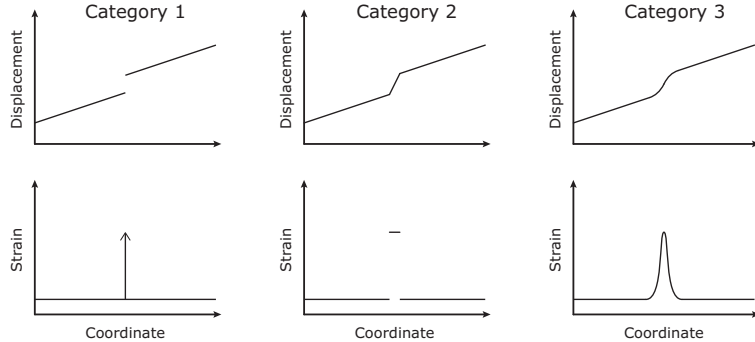


**Figure 1.** Schematic displacement and strain distribution for different categories of models to describe localized deformations. Reproduced from Jirásek [2].

based on so called damage mechanics [3]. A constitutive law within this class of method is chosen, here based on the work by Oliver et al. [4], although other choices would be equally applicable, for example plasticity based methods.

Damage mechanics is a constitutive theory that describes the progressive loss of material integrity due to propagation of material defects, e.g. microcracks, that on a macroscopic scale leads to degradation of material stiffness. One of the most central concepts that need to be introduced is the so called effective stress tensor  $\bar{\sigma}$  which is defined as the stress acting on the resisting area of the material. The stress observed on the macroscopic scale is then referred to as the nominal stress  $\sigma$  measured on a unit volume of material. These two stress measures are related by a property called damage. In its most general form, damage should be represented by a fourth order tensor, but here it is represented by a single scalar variable  $\omega$ , i.e. isotropic scalar damage. From this follows

$$\bar{\sigma} = \frac{\sigma}{1 - \omega} \quad (3)$$

and if the microscopic material is assumed to be linear elastic, a constitutive law can be written as

$$\sigma = (1 - \omega) \mathbf{C}_{\text{el}} : \boldsymbol{\epsilon}, \quad (4)$$

where  $\mathbf{C}_{\text{el}}$  is the elasticity tensor. Consequently, the entire non-linear response on the macroscopic scale is thus governed by the evolution of  $\omega$ . A loading function  $f$  is introduced that controls when  $\omega$  grows:

$$f(\boldsymbol{\epsilon}, \kappa) \equiv \tilde{\varepsilon}(\boldsymbol{\epsilon}) + \kappa \leq 0 \quad (5)$$

In Eq. (5),  $\tilde{\varepsilon}$  is a scalar measure of the strain level called the equivalent strain and  $\kappa$  is an internal variable. The definition of  $\tilde{\varepsilon}$  specifies the shape of the elastic domain, where in this study either of the definitions from Eqs. (6) and (7) has been used.

$$\tilde{\varepsilon} = \frac{1}{E} \max_{I=1,2,3} \langle \mathbf{C}_{\text{el}} : \boldsymbol{\epsilon} \rangle_I = \frac{1}{E} \max_{I=1,2,3} \langle \sigma \rangle_I \quad (6)$$

$$\tilde{\varepsilon} = \sqrt{\langle \boldsymbol{\epsilon} : \boldsymbol{\epsilon} \rangle} \quad (7)$$

Eq. (6) corresponds to a Rankine failure criterion where  $E$  is Young's modulus and the Macaulay brackets  $\langle \cdot \rangle$  denote the positive parts operator. Hence this definition only accounts for tensile failure. Equation (7) is the so called Mazars equivalent strain, which is often used for applications involving concrete [5]. In Mazars definition both tensile and compressive damage are considered. As for yield functions in plasticity, many other definitions of  $\tilde{\varepsilon}$  can be found in the literature [3].

The evolution of the elastic domain is controlled by a set of loading/unloading conditions on the Kuhn-Tucker form

$$f \leq 0, \quad \dot{\kappa} \geq 0, \quad \dot{\kappa} f = 0, \quad (8)$$

which implies that  $\kappa$  is the largest strain level reached by the material.

The last essential part of an isotropic damage model is a damage evolution law which defines the growth of  $\omega$  with respect to  $\kappa$ . A commonly used expression is the exponential function proposed by Oliver et al. [4] in Eq. (9), here used for tensile damage. Another choice is the function proposed by Mazars and Pijaudier-

Cabot [5] in Eq. (10), here used for compressive damage when Mazars equivalent strain is used.

$$\omega(\kappa) = 1 - \frac{\varepsilon_0}{\kappa} \exp\left(-\frac{\kappa - \varepsilon_0}{\varepsilon_f}\right) \quad (9)$$

$$\begin{aligned} \omega(\kappa) = 1 - \frac{(1 - A_c)\varepsilon_0}{\kappa} \\ - A_c \exp[-B_c(\kappa - \varepsilon_0)] \end{aligned} \quad (10)$$

In Eqs. (9) and (10),  $\varepsilon_0$  is the damage threshold while  $\varepsilon_f$  controls the slope of the strain softening curve in Eq. (9) while  $A_c$  and  $B_c$  controls the shape of the curve in Eq. (10).

When considering both tensile and compressive damage, a few additional equations are necessary to complete the model. These distinguish which damage mechanism is active, and also how to combine them if both are active. However, regardless a single scalar damage variable enters the constitutive law in Eq. (4).

### 3. Numerical considerations

Given the strain softening behaviour of quasi-brittle materials, using a constitutive law as the one outlined in section 2 would lead to a strong mesh dependency of the results. In fact, the solution would lack objectivity, meaning that the results do not converge to a single solution upon mesh refinement. This can be explained by the fact that at any given stress level below the peak load, two strain values satisfies the constitutive equation; either in the elastic or in the strain softening regime. If strains localize, it follows that the strain softening region will be as narrow as possible to minimize the amount of energy dissipated. In a FE context this corresponds to a single element or Gauss point, i.e. the amount of energy dissipated decrease with the element size. Two overcome this; two possible approaches are often mentioned [2]:

1. Use a stress-strain law that at each material point depends on the element size,
2. Add a localization limiter to the constitutive law so that the simulated localization zone corresponds to that observed experimentally.

#### 3.1 Local Model

The first approach corresponds to the so called Crack-band method [6] where the global

material behaviour is given by a stress-crack opening law. However, on the local level of each Gauss point, a unique stress-strain relationship is defined from this global behaviour by considering the local element size. The conversion from the global material behaviour is based on the width of the simulated localization zone at each specific point, the crack-band  $h_b$ . The difficulty in using this approach then becomes to determine a representative value of  $h_b$ , which for example might depend on the interpolation order, the size and shape of the element and the current stress state.

In Comsol, the most straightforward approach is to use the built-in element metric variable  $h$ . However, this variable always provides the longest element edge which likely is a poor estimation of  $h_b$ . A better approach might be to use the area  $A$  or volume  $V$  of each element to estimate  $h_b$ . While this would better account for the element shape, it does not consider the crack direction with respect to the element grid. Even for regular meshes this can have a significant impact on  $h_b$  as shown in Fig. 2a. Hence, in this study a method proposed by Cervenka et al. [7] to estimate  $h_b$  is used that considers the crack direction. The crack-band  $h_b$  is estimated by projecting the coordinates of the element nodal points on a crack plan given by principal strain directions. Then the largest distance between these projected points give  $h_b$ . This is schematically shown in Fig. 2b for a rectangular element in 2D.

When  $h_b$  has been determined, the unique stress-strain curve can be defined at that Gauss point. For example, if Eq. (9) is used,  $\varepsilon_f = G_f/(f_t h_b) + \varepsilon_0/2$  where  $f_t$  is the tensile strength and  $G_f$  the fracture energy.

#### 3.2 Non-local Model

A localization limiter enforces a more realistic and mesh-independent size of the strain softening region by supplying more information about the material structure to the constitutive law. One of the perhaps most widely used localization limiters is the concept of a non-local continuum. The most general form is the integral type formulation, where a variable is replaced by its weighted average over a spatial neighbourhood of each Gauss point [8]. Here, however, a differential version is used by

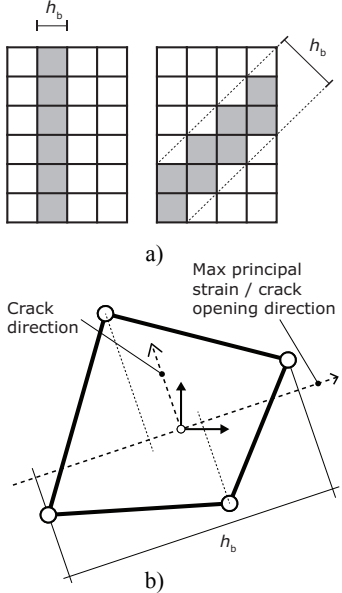


**Figure 2.** Effect of the crack direction on the simulated crack band (a). Schematic description of the projection method (b).

introducing higher-order gradients into the constitutive law following Peerlings et al. [9]. More precisely a so called implicit gradient model is adopted that introduces a non-local counterpart of the equivalent strain  $\bar{\varepsilon}$  as a solution to the Helmholtz equation.

$$\bar{\varepsilon} - c\nabla^2\bar{\varepsilon} = \bar{\varepsilon} \quad (11)$$

Parameter  $c$  in Eq. (11) has the dimensions of length squared and is thus related to the width of the localization zone. Equation (11) is then complemented with a natural boundary condition applied to the physical boundary of the structure

$$\nabla\bar{\varepsilon} \cdot \mathbf{n} = 0 \quad (12)$$

where  $\mathbf{n}$  is the surface normal. To complete the non-local constitutive law, the non-local variable  $\bar{\varepsilon}$  replaces its local counterpart in Eq. (5).

#### 4. Implementation in COMSOL Multiphysics®

The implementation in Comsol Multiphysics ver. 5.2 is done using a combination of the built-in features of the Solid Mechanics interface and equation-based-modelling. The isotropic scalar damage mechanics model in its stress-strain format is implemented by defining a nominal

stress measure that replaces the default stress measure (e.g. solid.s111) in the weak expression of the Linear Elastic material model. The default stress measure should then be interpreted as the effective stress as given by Eq. (3). To include the non-linear and history dependent response of the damage model an internal variable is needed, i.e.  $\kappa$ . This is set up as a domain ODE with the Gauss point data shape function and using the Previous Solution solver attribute to ensure that the loading/unloading conditions of Eq. (8) are met. The remaining parts, for example the equivalent strain measures from Eq. (6) or (7) and the damage evolution laws from Eq. (9) or (10), are implemented as variable definitions.

In defining the nominal stress tensor, an important aspect to account for is the unilateral character of damage. That is, damage is only active for certain stress states, for example if a tensile crack is compressed the effect of damage should be deactivated. Furthermore, such changes in compliance should appear without spurious stress jumps. This is here achieved by utilizing the spectral decomposition of the stress tensor into its principal components. For each effective principal stress  $\bar{\sigma}_i$  (e.g. solid.sp1) it is checked if damage is active and whether it is tensile or compressive. The principal nominal stresses  $\sigma_i$  can then be defined and next the nominal stress tensor  $\boldsymbol{\sigma}$  constructed under the assumption that the principal directions are unchanged.

The local crack-band model is appended by accounting for the characteristic element length  $h_b$  in the variable definition of  $\varepsilon_f$  as outlined in section 3.1. To define  $h_b$  using the projection method, information is needed about element coordinates and stress states (e.g. principal directions) at individual elements. This information is obtained using the built-in `atlocal` operator.

To implement the gradient enhanced version of the model outlined in section 3.2, a domain PDE is added to the model with the non-local equivalent strain  $\bar{\varepsilon}$  as the dependent variable. This is discretized using Lagrange shape functions, preferably of one order below the displacements, although not necessarily. The remaining modification required is as previously mentioned only in a single variable definition, the one which defines the internal variable  $\kappa$ .

In order to facilitate easier use of the implemented model, a custom physics interface including all the features described above has been built using the Physics Builder. This custom user interface must be used in conjunction with the Solid Mechanics node and the Linear Elastic material model.

## 5. Verification examples

To verify the model implemented in Comsol Multiphysics, a number of examples compared with experimental results are presented in the following. Both the local and non-local models are applied to cases of plain concrete, while the local model is also applied to a case of reinforced concrete with multiple cracks. For all examples, plane stress conditions are assumed and a Poisson's ratio of 0.2 is used. Additional examples showing the implemented model can be found in [10].

### 5.1 Plain concrete

First, to highlight the differences between the local and non-local models, a simple 1D example of a bar in uniaxial tension is analysed. The material is given a Young's modulus of 29 GPa and a tensile strength of 2.8 MPa using the Rankine criterion of Eq. (7). However, to force the strains to localize, the tensile strength of a single element in the midsection is reduced with 5 %. Furthermore, the bar is loaded using direct displacement control to allow the post-peak behaviour to be analysed. The local model needs an additional material property, the fracture energy, which is here set to 80 J/m<sup>2</sup>. Furthermore, a linear displacement field is used with an element size of 5 mm. The non-local model needs to be complemented with an internal length measure to control the width of the localization zone. Here done through parameter  $c$  that is set to 25 mm<sup>2</sup>. Then the stress-strain law used is calibrated so that approximately the same amount of energy as for local model is dissipated, i.e. 80 J/m<sup>2</sup>. The non-local model is set up with a quadratic displacement field, while the non-local strain  $\bar{\epsilon}$  is discretized with linear interpolation functions. An element size of 1 mm is used in order to obtain a better resolution of the results.

The load-deflection curves obtained from both models are shown in Fig. 3a. Additionally,

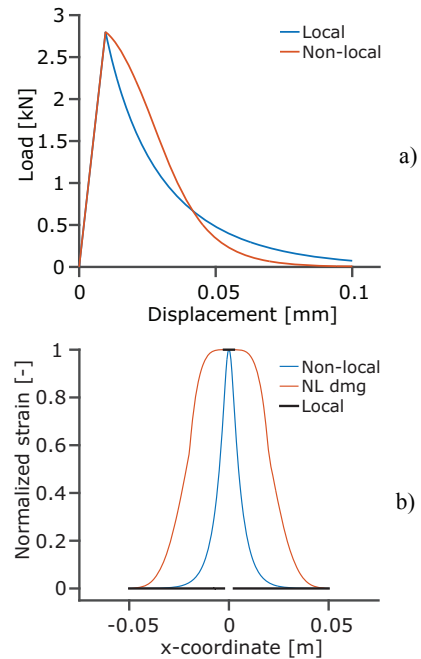


**Figure 3.** Load displacement curve (a) and strain-profiles along the bar (b) for the two models used.

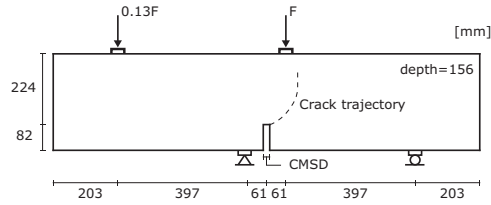


**Figure 4.** Geometry and boundary conditions of the 4-point shear test by Arrea and Ingraffea [11].

the strain profiles along the bar for the respective model are shown in Fig. 3b together with the damage profile of the non-local model. Looking at the strain profiles the difference between the two models is clear. As expected there is a distinct jump in the strain field of the local model where the crack is, while the strain field remain continuous for the non-local model.

The second example is of a notched concrete beam under 4-point loading tested by Arrea and Ingraffea [11]. The test setup is shown in Fig. 4, where the unsymmetric boundary and loading points are intended to produce a mixed mode fracture, resulting in the curved crack trajectory shown in the figure. The same material properties and discretization orders as for the uniaxial bar are used in this example. However, for both models an element size of 7.5 mm is

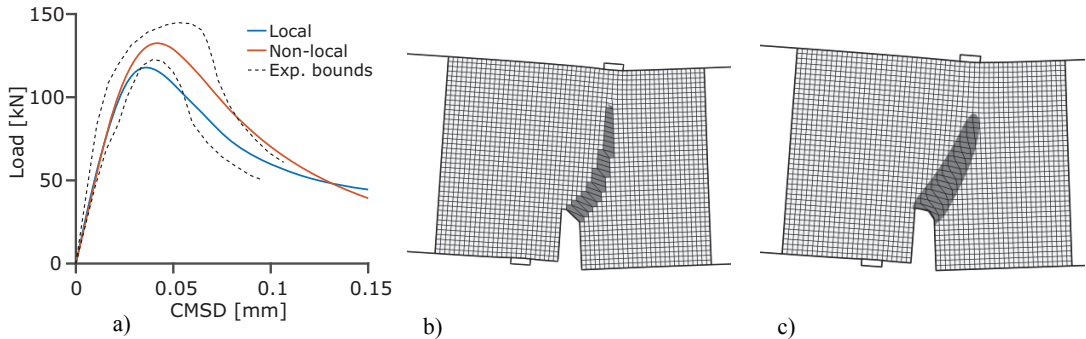


**Figure 5.** Load-CSMD curves (a) and simulated cracks for the local model (b) and the non-local model (c).

used. Since the post-peak behaviour of the beam measured at the load plates is highly unstable, it is necessary to use an indirect displacement control. The load level is thus set to increase linearly with the crack mouth sliding displacement (CMSD) from Fig. 4.

The load-CSMD curves obtained for both models are shown in Fig. 5a, in comparison with the experimental results. Given the unstable behaviour of the problem, both models can be said to be in good agreement with the experiments. However, the local model slightly underestimates the peak load, while the non-local model gives an excellent prediction. A reason for this could be the difference in the obtained crack trajectories as seen in Figs. 5b and 5c, where that of the local model is steeper. From these two figures it is also clear that the crack pattern obtained from the local model is more influenced by the element grid.

## 5.2 Reinforced concrete

To show that and how this type of model can be successfully used for reinforced concrete, a beam from an experimental series by Leonhardt [12] is analysed. The chosen beam has a high amount of flexural reinforcement (geometrical content of 1.7 %) and is expected to exhibit a shear type failure, with an inclined crack causing the ultimate failure. The dimensions of the beam are shown in Fig. 6, which also includes the observed crack pattern. Only the local model has been used for the concrete, here using Mazars equivalent strain definition from Eq. (7). It is given a Young's modulus of 24 GPa, a tensile strength of 2.2 MPa, a fracture energy of 100 J/m<sup>2</sup> and a compressive strength of 29 MPa.

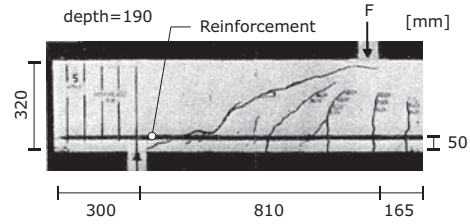


**Figure 6.** Geometry and boundary condition of the reinforced concrete beam tested by Leonhardt [12], including the observed crack pattern.

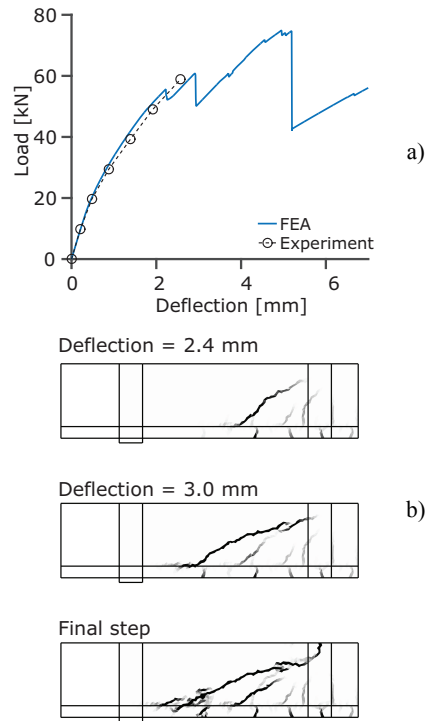


**Figure 7.** Load-deflection curve (a) and simulated crack patterns at different load levels (b).

To minimize the mesh bias of cracks, a triangular grid is used with an approximate element size of 15 mm. The longitudinal reinforcement is modelled using truss elements with a Young's modulus of 208 GPa which remain in the elastic range throughout the simulation. Furthermore, the truss elements are constrained to follow the displacements of the concrete. Only linear displacement fields are considered for both materials. Lastly, it should also be mentioned that a symmetry plane is utilized and that the load here is applied using displacement control.

The obtained load-deflection curve is shown in Fig. 7a and compared with the available experimental data. The first significant drop in the simulated curves appears at approximately 60 kN and a deflection around 2.9 mm where the first major diagonal crack appears. It should here be mentioned that this drop is reported as the ultimate load capacity in the experiments. However, in the simulation, the load level can be increased further up to around 75 kN where the shear crack grows further and also crushing of the concrete start to occur under the load plate. The different stages of cracking are shown in Fig. 7b, which is in fairly good agreement that observed experimentally.

## 6. Conclusions

A model has been presented that enhances the solid mechanics features of Comsol Multiphysics to include the analysis of localized deformations due to cracking of quasi-brittle materials such as concrete. This is done by adopting an isotropic scalar damage constitutive law combined with two different regularization techniques to ensure mesh objectivity.

These two techniques are compared using examples of plain concrete where single cracks can be studied. Both models show good agreement when compared to experimental data. The local crack band model is also applied to a reinforced concrete beam, exhibiting a more complex crack pattern. Also for this example, the model shows good agreement with experimental results.

## 7. References

1. ZP Bažant, Size Effect in Blunt Fracture: Concrete, Rock, Metal, *J. Eng. Mech.*, **110**, 518-35 (1984)
2. M Jirásek, *Modeling of localized inelastic deformation*, Lecture notes, Czech Technical University, Prague, Czech Republic (2014)
3. J Lemaitre, *A Course on Damage Mechanics*, 2nd ed., Springer, Berlin, Germany (1996)
4. J Oliver, M Cervera, S Oller and J Lubliner, Isotropic damage models and smeared crack analysis of concrete, In: *Proceedings of SCI-C 2*, 945-57, Zell am See, Austria (1990)
5. ZP Bažant and B. Oh, Crack band theory for fracture of concrete, *Matériaux et Construction*, **5**, 155-77 (1983)
6. J Mazars and G Pijaudier-Cabot, Continuum Damage Theory —Application to Concrete, *J. Eng. Mech.*, **115**, 345-65 (1989)
7. V Cervenka, R Pukl, Z Ozbolt and R Elsgehausen, Mesh sensitivity effects in smeared finite element analysis of concrete fracture, In: *Proceedings of FraMCoS-2*, 1387-96, Freiburg, Germany (1990)
8. G Pijaudier-Cabot and ZP Bažant, Nonlocal Damage Theory, *J. Eng. Mech.*, **113**, 1512-33 (1987)
9. RHJ Peerlings, R De Borst, WAM Brekelmans JHP De Vree, Gradient enhanced damage for quasi-brittle materials, *Int. J. Numer. Meth. Eng.*, **39**, 3391-403 (1996)
10. T Gasch, *Concrete as a multi-physical material with applications to hydro power facilities*, Lic. thesis, KTH Royal Institute of Technology, Stockholm, Sweden (2016).
11. M Arrea and AR Ingraffea, *Mixed-mode crack propagation in mortar and concrete*, Cornell University, Ithaca, USA (1982)
12. F Leonhardt, *On the reduction of shear reinforcement as derived from the Stuttgart shear tests 1961-1963*, IABSE congress report 7, (1964)

## 8. Acknowledgements

The research presented was carried out as a part of “Swedish Hydropower Centre -SVC”. SVC has been established by the Swedish Energy Agency, Energiforsk and Svenska Kraftnät together with Luleå University of Technology, KTH Royal Institute of Technology, Chalmers University of Technology and Uppsala University. [www.svc.nu](http://www.svc.nu).